Physical Review & Research International
1(3): 106-115, 2011

SCIENCEDOMAIN *international*
www.sciencedomain.org

Assessment of Heat Flow Stability Profiles in Response to Non-Linear Thermal Potential

C. I. Okoro[1] and M. Y. Onimisi[1*]

[1]Department of Physics, Nigerian Defence Academy, P.M.B 2109, Kaduna, Nigeria.

Research Article

Received 25th May 2011
Accepted 27th June 2011
Online Ready 3rd July 2011

ABSTRACT

Heat flow stability profiles in the presence of external thermal field require careful qualitative treatment. The computational data must be considered to agree with realistic models. A hexagonal plate endowed with the thermal and material properties of a pure metal was chosen as test case and finite element algorithm was employed to obtain the numerical solutions of the temperature distributions. This was simulated with the aid of Matlab tool. Result shows that the radiation and logarithmic potentials have no disturbance on the stability profiles when compared with a control model. Classically, the circular orbits result in the event that the total internal thermal energy equals the global minimum of the applied potential. It is thus predicted that adjustment of the computational data would influence the entropy profiles of the system which in turn distorts the stability profiles in a stochastic manner.

Keywords: Thermal potentials; control model; stability profiles; saddle points; finite element algorithm;

NOMENCLATURE

*A: Area, m**2; E: Surface emissivity, dimensionless;* α*: Thermal conductivity, J/sec/m/K;* κ *Thermal diffusivity, m**2/sec; n: Number of nodes;* N_e^n *Element shape function for node n, element e; H: Extended heat source, W/ m**3/sec;* H_p*: Point heat source, W/ m**3/sec;* R_e *External force; t: Time, sec;* θ *: Temperature field, K;* $\bar{\theta}'$ *Temperature derivative wrt position, K/m;*

**Corresponding author: Email: onimisimy@yahoo.com;*

1. INTRODUCTION

Computer simulation of physical phenomena has significantly improved the agreement between theoretical predictions and experimental results. Ranging from numerical capability, error minimization, stability and convergence of solutions, the use of computers in solving physical and engineering problems is overwhelming.

In most problems of continuum physics and potential theory, the analysis of the stability profiles of systems is of great interest in application. Molecular dynamics study of flow profile of a gas flowing along a surface has been shown to depend on its wettability at the surface (Markvoort et al., 2005). The wetting agent, here in referred to, plays the role of the thermal potential at the boundary.

In physics terms, stability means, roughly, that a small disturbance of a physical system at some instant changes the behavior of the system only slightly at all finite times (Erwin, 2005).This is directly associated with the equilibrium profiles of the system. In principle, stable equilibrium may occur if a small disturbance results in locally bounded region (Herbert et al., 1950). But when the applied field is considerably large, a qualitative region of unstable equilibrium would be observed. When such arises, the flow packet is stagnant and any slight disturbance will result in locally unbounded region. At the point of stability the circular orbits result in the event that the total internal thermal energy is in equilibrium with the global minimum of the applied potential. Statistically, the packets in the neighborhood of the potential begin to respond to the applied potential by vibrating with increasing amplitudes. Results have shown that the magnitude of the thermal boundary layer attains a critical value (Lyubimov et al., 2011). Gradually, the packets progressively farther up the material, increasing their amplitudes of vibration until those at the associated end are reached. This increased disturbance results in an increase in temperature of the material conductor.

Interestingly, studies have shown and confirmed the existence of the quantum mechanical zero-point energy. In the study of electromagnetic field fluctuations (Theodore, 1948), it was cited that the displacement of the 2S level of hydrogen can be simply explained as a shift in the energy of the atom arising from its interaction with the radiation field. It was rightly observed that the radiation field in the empty space gives rise to fluctuating electric and magnetic fields. In a more recent study (Rueda et al., 1995), it was confirmed that the zero-point energy applies to all interactions, except gravitational interactions. These studies clearly justify the possibility of the zero point effect due to the interactions of the thermal fields, most especially the radiation field.

In this study we have attempted to predict the existence of the zero-point energy as an agent for the meta-stable to stable transition of the heat flow profile. Also we have assessed the influence of radiation and logarithmic thermal potentials by qualitative treatment. This is studied over a pure metallic plate with an arbitrary hexagonal geometry. We have adopted the computational data used in our earlier work (Okoro, 2011, unpublished M.Sc. thesis) and have made little modification.

2. THE MATHEMATICAL PROBLEM

We consider an arbitrary volume V lying within the solid plate and bounded by a surface S as shown below.

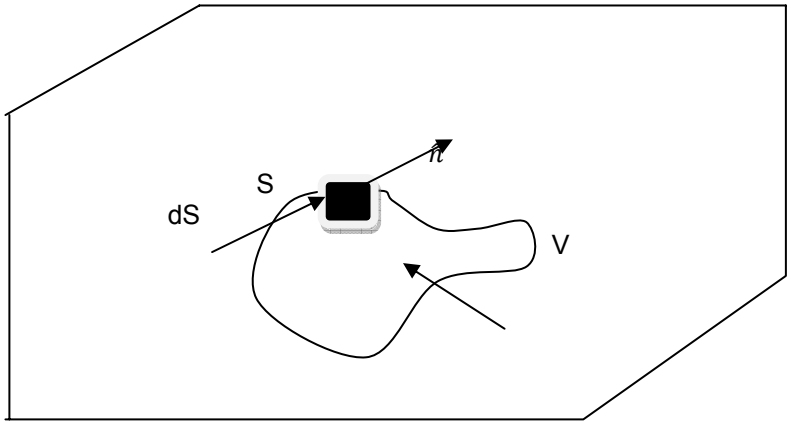

Fig. 1. Arbitrary volume V bounded by the surface S

For steady state flow in the presence of heat sources, the heat flow is modeled as the familiar 2-dimensional Poisson's equation:

$$\nabla^2\theta = \frac{1}{k}(H + H_p\delta(r - r_p)) \tag{1}$$

The boundary potentials employed are

$$\frac{\partial\theta}{\partial n} = \begin{cases} 0, \text{ control model} \\ 4\mathrm{E}\sigma\theta_r^3(\theta - \theta_r), \text{ radiationpotential} \\ \frac{-\alpha\theta}{\beta}\ln(1 + \frac{\beta g}{K_o\theta_o}) \text{ , logarithmic potential} \end{cases} \tag{2}$$

The boundary temperatures are shown on table 2.

3. DERIVATION OF THE 2D FINITE ELEMENT SCHEME

We now seek to derive the 2D finite element scheme for equation (1) from which the temperature field evolves within the minimum computational error.
Consider the minimization problem:

$$dI = \int_A (\frac{\partial F}{\partial\theta}\, d\theta + \frac{\partial F}{\partial\bar{\theta}} d\bar{\theta})\mathrm{dA} = 0 \tag{3}$$

Where F is a particular integrand which minimizes the functional for the integral I.

The general functional for the 2-dimensional heat flow is

$$\mathrm{F(x, y, \theta, \bar{\theta})} = \frac{1}{2}\sigma\left[\left(\frac{\mathrm{d}\theta}{\mathrm{dx}}\right)^2\right] - \frac{1}{2}\mathrm{Q}\theta^2 + \frac{1}{\kappa}\mathrm{H}\theta \tag{4}$$

Where σ is a constant.

$$\frac{\partial F}{\partial \theta} = -QT + \frac{1}{\kappa}\mathrm{H}; \frac{\partial F}{\partial \bar{\theta}} = \sigma \frac{\mathrm{d}\theta}{\mathrm{dx}} \tag{5}$$

Substituting Eq. (5) into Eq.(3) we have;

$$dI = \int_{S_1}^{S_2} \left(-Q\theta + \frac{1}{\kappa}\mathrm{H}\right) d\theta \mathrm{dS} + \int_{\mathrm{S}_1}^{\mathrm{S}_2} \sigma \frac{\mathrm{d}\theta}{\mathrm{dx}}\ d\bar{\theta}\mathrm{dS}, \lim_{\Delta x \Delta y \to 0} dA = dS \tag{6}$$

Performing integration by parts on the second integral in Eq. (6) and then integrating the resulting differential yields

$$I = \iint_A \frac{1}{2}\sigma \nabla^2 \theta dA + \int_S \frac{1}{2} Q\theta^2 dS - \iint_A \frac{1}{k} H\theta dA \tag{7}$$

For some edge S over which the plate thermally interacts with the surrounding.
In an effort to develop the finite element model, a linear interpolation was considered and an appropriate shape function has been chosen.

$$N_e = \frac{A_e}{A}, \text{i=1,2,3} \tag{8}$$

Since element strains are obtained by taking the derivatives with respect to the Cartesian coordinates, we have the following relations;

$x = \sum_{e=1}^{3} N_e\, x_e; y = \sum_{e=1}^{3} N_e\, y_e; x = \sum_{e=1}^{3} q_e\, x_e; y = \sum_{e=1}^{3} q_e\, y_e; u = \sum_{e=1}^{3} q_e\, u_e;$

$v = \sum_{e=1}^{3} q_e\, v_e$

$q_1 = 1 - r - s, q_2 = r, q_3 = s$, provided $\sum_{e=1}^{3} q_i = 1$. The evaluation of the element matrices now involves a Jacobian transformation and all integrations carried out on the natural coordinates, i.e. r's integrations go from 0 to 1 and the s integrations go from 0 to (1-r).The Jacobian, generalized element temperature and the temperature-gradient interpolation matrices, respectively are;

$$J^e = \begin{pmatrix} \frac{\partial x}{\partial r} & \frac{\partial y}{\partial r} & \frac{\partial z}{\partial r} \\ \frac{\partial x}{\partial s} & \frac{\partial y}{\partial s} & \frac{\partial z}{\partial s} \\ \frac{\partial x}{\partial t} & \frac{\partial y}{\partial t} & \frac{\partial z}{\partial t} \end{pmatrix} \tag{9}$$

$$Q^e = \begin{pmatrix} q_1 & 0 & q_2 & 0 & q_3 & 0 \\ 0 & q_1 & 0 & q_2 & 0 & q_3 \end{pmatrix} \tag{10}$$

$$B^e = \begin{pmatrix} \frac{\partial q_1}{\partial x} & 0 & \frac{\partial q_2}{\partial x} & 0 & \frac{\partial q_3}{\partial x} & 0 \\ 0 & \frac{\partial q_1}{\partial y} & 0 & \frac{\partial q_2}{\partial y} & 0 & \frac{\partial q_2}{\partial y} \\ \frac{\partial q_1}{\partial y} & \frac{\partial q_1}{\partial x} & \frac{\partial q_2}{\partial y} & \frac{\partial q_2}{\partial x} & \frac{\partial q_3}{\partial y} & \frac{\partial q_3}{\partial x} \end{pmatrix} \tag{11}$$

Thus the element stiffness matrix is computed as

$$K^e = \mathrm{h} \iint B^{(e)T} C B^e |J^e| dA \tag{12}$$

The extended heat source, the differential boundary condition and the point sources are computed respectively as;

$$R_H^e = \text{h}\iint Q^{(e)T} H|J^e|dA; \quad (13)$$

$$R_S^e = \int_S Q^{(e)T} \frac{\partial\theta}{\partial n}|J^e|ds\,; \quad (14)$$

$$R_p^e = \sum_e Q^{(e)T} H_p \frac{\theta_p}{k} \quad (15)$$

Using the principle of virtual temperature and assembling the element matrices we obtain

$$K\theta = R_H + R_S + R_P \quad (16)$$

4. SIMULATION TEST CASE

Our test plate was modeled with 34 nodes and 48 triangular elements spanning the entire domain. We have also considered point source of strength 2×10^5 situated at nodes 7 and 30. A uniform extended source of strength 10^6 has been applied and the following were used. The potential is applied at nodes 17, 24 and 31. These nodal points have been strategically chosen to enable symmetry and homogeneity.

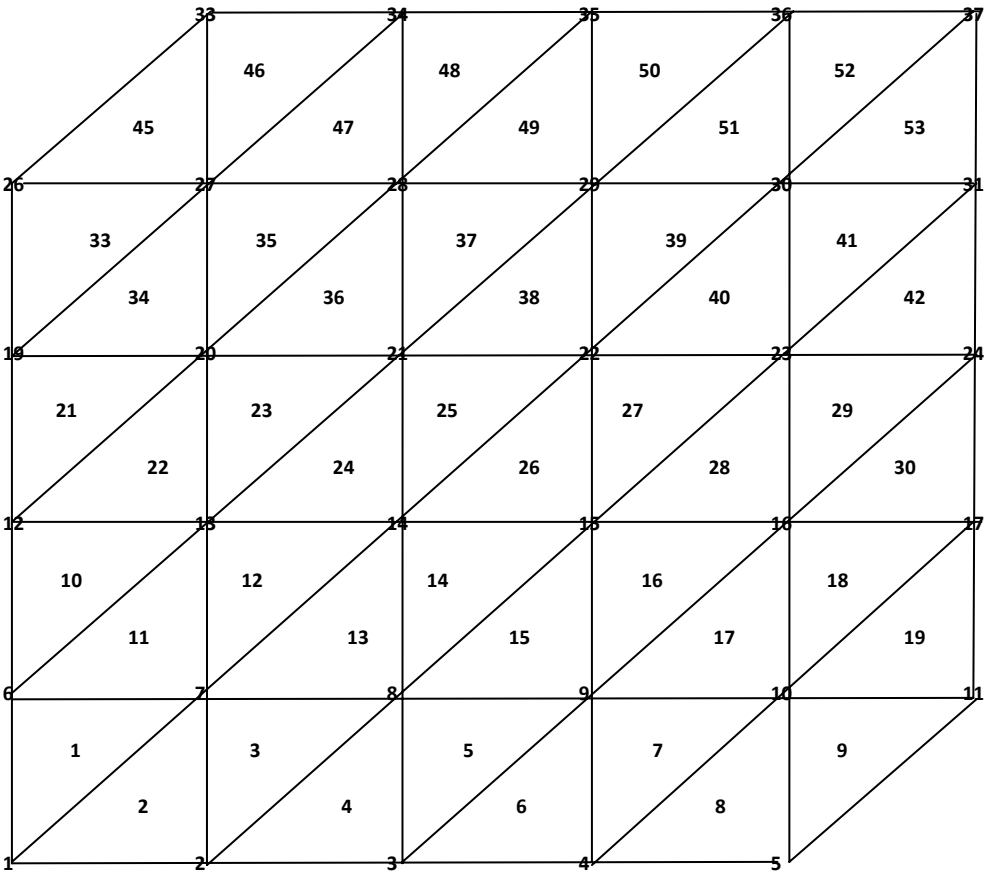

Fig. 2. The finite element discretization of the simulation plate

Also, we have considered the presence of a uniform extended source of strength 10^6 throughout the heat flow domain. The physical situation of our simulation domain is shown in figure 2 as well as the data we have used for computation.We have carried the simulation using the following forms of thermal potentials in Eq. (2).

5. ASSUMPTIONS AND DATA

While computing the finite element algorithms, we have made the following assumptions:

- The mean temperature was taken to be the average of the fixed boundary temperatures. That is;
- $$\bar{\theta} = \frac{800+700+700+500}{4} = 675K \quad (17)$$
- The lower temperature limit for the evaluation of the g function was arbitrarily assumed to be 300K, provided $\theta_o \leq$ the least possible temperature obtainable $(\theta_{\min})$,
- We have retain the non-vanishing behavior of the logarithmic potential by establishing the inequality;
- $$\beta g > \theta_o K_o \quad (18)$$

To preserve this inequality we have assumed the value of β to be unity.

- The g function was evaluated using the equation (Kane et al., 1990);

$$g = \int_{\theta_o}^{\bar{\theta}} K(\theta) d\theta \quad (19)$$

Substituting the values above into the equation and evaluating the integral we obtain

$g = 4.0 \times 10^5$

Also we have used the following data from ref. [5]: A=0.02;σ =5.67$\times 10^{-8}$; $\mathrm{H_p} = 2 \times 10^5$; $\mathrm{H} = 10^6$; $\kappa = 2 \times 10^3$; $K_o = 10$; $|J^e|$=0.04;β=1.0;E=0.96;α=3.0;d=0.2;g=4.0$\times 10^5$; $\bar{\theta} = 675K$; $\theta_{\mathrm{r}} = 820K$; $\theta_o = 300K$;

6. RESULTS

The finite element algorithm was employed to simulate the heat flow on a hexagonal pure metallic plate as a test case. The responses of the model to variants of boundary formulations have been demonstrated using linear, power and logarithm laws. All computations were carried out manually and the simulation views were generated using MATLAB 7.5.0 graphic features with a Window XP operating system in single precision. In order to assess the effects of these variants of boundary formulations, we have also computed the control model.

Table 1. Computed temperatures against node numbers for the radiation potential, logarithmic potential and control model

Node numbers	Radiation law Temperature (K)	Logarithmic law Temperature (K)	Control model Temperature (K)
7	700.75	700.75	712.50
8	801.71	801.71	741.67
9	800.75	800.75	749.67
10	790.00	790.00	700.00
13	734.45	734.45	708.33
14	821.29	821.29	739.42
15	821.29	821.29	739.42
16	742.84	742.84	749.20
17	699.94	699.94	747.30
20	734.42	734.42	708.33
21	804.06	804.06	733.34
22	809.97	809.97	738.78
23	760.56	760.56	742.82
24	837.20	1035.88	741.55
27	706.38	706.38	697.35
28	597.06	597.06	714.55
29	597.04	597.66	660.77
31	*514.23*	1150.94	680.33

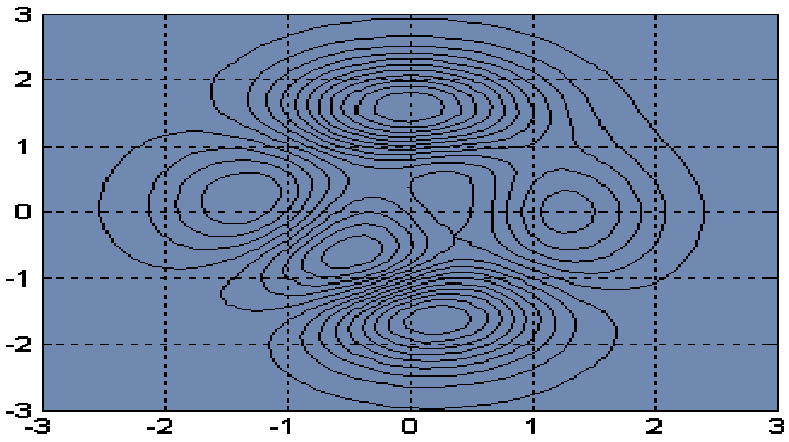

Fig. 3. The first 20 contour plots for the radiation potential

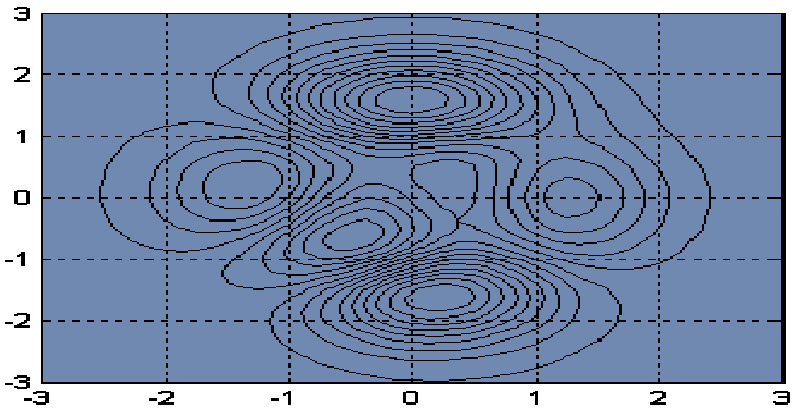

Fig. 4. The first 20 contour plots for the logarithmic potential

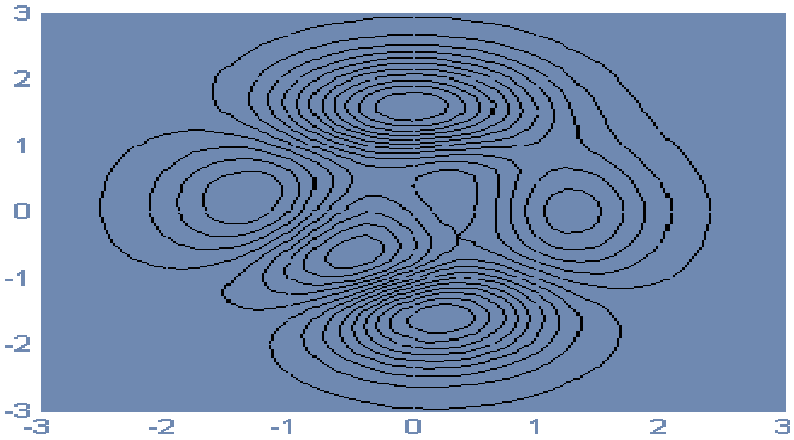

Fig. 5. The first 20 contour plots for the control model

Table 2. Fixed boundary temperatures against node numbers for test and control models

Node numbers	Temperatures (K)
1	750.00
2	800.00
3	800.00
5	800.00
11	750.00
12	700.00
16	700.00
19	700.00
26	700.00
33	500.00
35	500.00
36	500.00
37	600.00

7. DISCUSSION

The results obtained of the heat flow system (Table 2) have been shown not to give sufficient information about the stability profiles, in response to the applied boundary potentials. The qualitative treatments (Figures 3, 4 and 5) have shown quite some similar results. The induced thermal fields have been found to be insufficient to destabilize the critical point. There are two reasons for this. The computational data must be varied in order to produce significant disturbance to the stability profiles. The other reason is that heat flow pose spontaneous internal thermal energy which can only be distorted by a considerably stronger interacting potential.

From the qualitative results obtained (Figures 3, 4 and 5), the locally bounded regions show stable equilibrium due to mall disturbance of the thermal field by the applied boundary potentials in Eq. 2. The unbounded regions indicate unstable equilibrium. In this case, slight disturbances by the applied potentials distort the stability regions and the entropy is higher than in the bounded regions, the degree of the entropy correlating positively with the magnitude of the applied potential. These results are in agreement with the theoretical treatments discussed by Herbert (Herbert et al., 1950).

Also, circular orbits have been observed (Figures 3, 4 and 5). This confirms the tendency of stable equilibrium. However, the circular orbit implies stable equilibrium only in the event that the minimum of the applied potential is in thermal equilibrium with the net internal thermal energy of the system. So-to-speak, information about the circular orbit is not sufficient to guarantee stability. More importantly is that our results confirm the existence of saddle point in the interior of the heat flow domain as shown by (Lyubimov et al., 2011).

Additionally, the heat flow profiles pose multiple connectivity (Figures 3, 4 and 5). This behavior in the zone condensation strategy was employed in the work (Kane et al., 1990). It is implored that the zone condensation be handled with great care, not to violet the symmetry of the system as well as the homogeneity of the heat flow.

It is imperative to note that classical treatment of the heat flow stability profiles gives information of the stable and unstable equlibria. In terms of the meta-stable profile or the “meta-stable to stable transition”, it is predicted that the zero-point energy, due to the internal thermal energy of the system, exists. This is in agreement with earlier studies (Theodore, 1984, Rueda et al., 1995).

8. SUGGESTIONS

Based on the multiple connectivity observed, it is suggested that careful qualitative examination should be carried out prior the zone condensation strategy. The condensed thermal zones may be employed even for heterogeneous medium by understanding of the stability profiles. In particular, we suggest that an n-fold connected system be condensed into n-1 thermal zones.

Also, it is suggested that the meta-stable profile of the thermally interacting fields be treated as a quantum-mechanical effect.

9. CONCLUSION

It is predicted that adjustment of the computational data would influence the entropy profiles of the system which in turn distorts the stability profiles in a stochastic manner. Also, it is predicted that the zero-point energy plays a vital role in the stability of the thermally interacting systems.

ACKNOWLEDGEMENT

The authors desire to express their sincere appreciation for the encouragement, interest and constructive criticism given them by Professor S. S. Duwa. The work here reported was supported in part by Nigerian Defence Academy, Kaduna, Nigeria.

REFERENCES

Erwin, K. (2005). Advanced Engineering Mathematics 8th edition, Chapter 3. John Wiley and Sons. ISBN 9971-51-283-1.

Herbert, G., Charles, P., John, S. (1950). Classical Mechanics 3rd Edition. Addison Wesley, ISBN 0-201-65702-3.

Kane, J.H., Kumar, B.L.K., Saigal, S. (1990). An arbitrary multi-zone condensing technique for boundary element design sensitivity analysis. AIAA J., 28, 1277-1284.

Lyubimov, D., Lyubimov, D. T., Amiroudine, S., Beysens, D. (2011). Stability of a thermal boundary layer in the presence of vibration in weightlessness environment. European physics journal. Special Topics, 192, 129-134.

Lutz, H. (1970). The sea surface temperature deviation and the heat flow at the sea-air interface. Springer link-boundary-layer meteorology. 1, 3.

Markvoort, A.J., Hilbers, P.A.J., Nedea, S.V. (2005). Molecular dynamics study of the influence of wall-gas interactions on heat flow in nanochannnels. APS, Physical review E 71, 066702.

Rueda, A., Haisch, B., Cole, D.C. (1995). Vacuum zero-point field pressure instability in astrophysical plasma and the formation of cosmic voids. Astrophysical J., 445, 7-16.

Theodore, A.W. (1948). Some observable effects of the quantum-mechanical fluctuations of the electromagnetic field. Physical Rev., 74(9), 1157-1167.